Synthesis and Stabilization of Silver Metallic Nanoparticles and Premetallic Intermediates in Perfluoropolyether/CO_2 Reverse Micelle Systems

M. Chandler McLeod,[†] R. S. McHenry,[†] Eric J. Beckman,[‡] and Christopher B. Roberts*,[†]

Department of Chemical Engineering, Auburn University, Auburn, Alabama 36849, and Chemical Engineering Department, University of Pittsburgh, Pittsburgh, Pennsylvania 15261

Received: August 12, 2002; In Final Form: December 30, 2002

This article presents the stabilization of silver nanoparticle intermediates synthesized in ammonium perfluoropolyether (PFPE-NH_4) reverse micelles with supercritical fluid (SCF) carbon dioxide solvent as the continuous phase. Specifically, the intermediates were formed by the reduction of silver nitrate salt ($AgNO_3$) encapsulated within PFPE-NH_4 reverse micelles. The effect of reducing agent type, reverse micelle water content, water core buffering, and bulk solvent type were all investigated as factors affecting stabilization of the silver nanoparticle intermediates. Particles were characterized by in situ UV−visible spectroscopy and transmission electron microscopy (TEM). The UV−vis spectrum of these nanosized silver particles is sensitive to particle size, and thus time-resolved spectral measurements were utilized as a means of monitoring both intermediate growth and persistence. The silver intermediates were stabilized in PFPE-NH_4 reverse micelles as indicated by multiple UV−vis absorption bands that persist for periods of time measured to greater than 9 h. Intermediate stabilization is facilitated by a unique environment existing specifically as a result of PFPE-NH_4 surfactant presence and its local water environment in the reverse micelle rather than any effects arising from the carbon dioxide solvent.

Introduction

Nanomaterials are currently the focus of a large amount of research as they show potential in applications spanning from catalysts to sensors and optical materials, among others. Controlled organic synthesis as well as formation of metallic and semiconductor crystallites has been widely demonstrated in conventional liquid hydrocarbon solvents by exploiting reverse micelles as nanoscale reaction environments.[1−5] These unique environments result from thermodynamically stable organization of amphiphilic surfactants, which encapsulate a nanosized water core in contact with the hydrophilic headgroups of the surfactants. The hydrophobic tails of the surfactant are solvated by a bulk continuous-phase solvent. When water-soluble polar and ionic substances are dissolved within the reverse micelle water core, the continuous-phase solvent is left essentially unaltered. As a result, reactions involving the dissolved substances occur locally in the reverse micelle cores. Consequently, the size of the reverse micelle water core plays an important role in their application to nanomaterial synthesis brought about by controlled reactions in the water core. The size of the micelle core can be characterized by a W value that expresses the ratio of moles of water to moles of surfactant in the system ($W = [H_2O]/[\text{surfactant}]$).

Formation of nanometer-sized particles by metal ion reduction within reverse micelle water cores has been demonstrated for copper, silver, and other metals in numerous studies.[2−4,6,7] The nanoparticle growth process within the reverse micelles consists of a combination of intra- and intermicellar mechanisms. Upon addition of reducing agent to the microemulsion, the metal ions within each reverse micelle are rapidly reduced to their ground state. Subsequently the nanoparticle growth occurs by collision among micelles, which may then exchange water core contents, leading to further particle growth.[2,5,8−10] This process of exchange and growth continues until the particles reach a terminal size determined by the system and where the surfactant aids in stabilization of the particles.

Several papers have focused in detail on the production of metallic copper and silver nanoparticles by simple reduction reactions within the cores of AOT reverse micelles in normal liquid alkane solvents.[11−14] These studies revealed that the size of metallic particles after a fixed reaction time was influenced primarily by the intermicellar exchange rates dictated by the water content of the micelle, W, the average number of metal ions and reducing agent molecules per micelle, and the continuous-phase solvent type. Lisiecki and Pileni[13] and Bagwe and Khilar[8,9] found that the solvent properties can play an important role in the dynamics of nanoparticle formation because of the different interactions between the solvent and the surfactant tails, and hence they can influence the attractive interaction between micelles. Furthermore, Cason et al.[6] found that copper particle growth rates within AOT/alkane reverse micelles increased as a consequence of increased water content but that essentially the same particle size was eventually approached at all water contents in a given solvent. More importantly, it was found that the bulk solvent type had a significant influence on the copper particle growth rates and terminal particle size. In light of this solvent effect on nanoparticle growth, the ability to easily change the bulk solvent properties for desired particle characteristics appears promising and can be realized by supercritical fluids with their highly tunable nature. Variations in supercritical fluid solvent properties such as density, diffusivities, capacity for solutes, compressibility, and dielectric constant, among others, can be effected

* To whom all correspondence should be addressed: e-mail croberts@eng.auburn.edu.
[†] Auburn University.
[‡] University of Pittsburgh.

10.1021/jp0218645 CCC: $25.00
Published on Web 03/06/2003

by changes in temperature and pressure.[15] These adjustable properties thereby allow for regulation of reverse micelle collision rates and, consequently, particle growth rates.[7] Additionally, separation of the particles from the solvent is facilitated by the ease with which the supercritical solvent can be expanded away from the nanoparticles.

Supercritical fluids were first employed as a medium for reverse micellar reactions by Matson et al.[16] for the production of spherical aluminum hydroxide particles in supercritical propane. However, since this inception of supercritical fluids as a medium for reverse micelle reactions and particle formation, most research has continued to focus on the synthesis of particles in liquid systems. More recently, Cason et al.[7] have investigated the production of silver and copper nanoparticles in compressed and SCF alkanes to show that these solvents provide effective media for nanoparticle synthesis. Moreover, Parag et al.[17] recently demonstrated the importance of solvent density as a means of balancing steric repulsion forces and attractive van der Waals forces in order to achieve dispersion of dodecanethiol-coated gold and silver nanoparticles in supercritical ethane.

It would be desirable, however, to replace the flammable, expensive alkane solvent with supercritical CO_2 exactly because of its benign, inexpensive nature combined with its tunable solvent properties. Unfortunately, numerous surfactants have been shown to be relatively insoluble in sc-CO_2.[18] Researchers have, however, recently overcome this obstacle by employing surfactants with a fluorinated, CO_2-philic tail and a water-soluble headgroup for use in sc-CO_2/water microemulsions.[19−26] These surfactants have proven capable at forming reverse micelles in supercritical CO_2 and have been shown to effectively solvate water-soluble compounds in their bulk water core.

Johnston and co-workers[19,20] formed reverse micelles in sc-CO_2 bulk solvent by utilizing an ammonium carboxylate perfluoropolyether (PFPE) having the formula $CF_3O[CF_2CF(CF_3)O]_3CF_2COO^-NH_4^+$. Various probing techniques such as Fourier transform infrared (FTIR), UV−vis, X-band electron parametic resonance (EPR), and time-resolved fluorescence depolarization have been used to characterize the nature of the PFPE/CO_2 reverse micelles. EPR identified the micelle as having a bulklike water core able to solubilize ionic species while time-resolved fluorescence depolarization revealed an anisotropic/nonspherical reverse micelle.[27] FTIR and UV−vis spectroscopy by Johnston and co-workers[19,20] showed that the sc-CO_2/water microemulsion consists of regions of "bulk" hydrogen-bonded water, "interfacial" water, and "free" water dissolved in sc-CO_2. The UV−vis spectroscopy used methyl orange and indicated that the PFPE/sc-CO_2/water reverse micelle cores have a polar environment as seen in dry PFPE reverse micelles, a bulklike water region, and an acidic environment resulting from carbonic acid formation. da Rocha and Johnston[28] measured the interfacial tension at the water−CO_2 interface and determined that the area per surfactant at the water−CO_2 interface is considerably larger than the area per surfactant measured at water−oil surfaces. This results from a much smaller interfacial tension to be overcome at the water−CO_2 interface and also from the greater entropic contribution to the monolayer free energy resulting from increased penetration of the small CO_2 molecules into the tail region relative to larger oils. Additionally, Lee et al.[29] observed the interaction strength between droplets to be larger in water-in-CO_2 relative to water-in-oil microemulsions due to stronger tail−tail interactions resulting from the weak solvation by CO_2. As a result, it is more difficult to overcome droplet interactions to produce stable microemulsions. Finally, SANS measurements performed by Zielinski et al.[30] show evidence of a water-in-CO_2 microemulsion with a droplet radius ranging from 20 to 36 Å.

Holmes et al.[31] have demonstrated compartmentalized production of cadmium sulfide Q-particles in PFPE/sc-CO_2 microemulsions by reaction of cadmium nitrate with sodium sulfite. Wai and co-workers[32−34] have more recently synthesized metallic silver and copper nanoparticles within sc-CO_2 microemulsions formed from a surfactant mixture of both phosphate-functionalized PFPE and sodium AOT.

This paper presents the results of an investigation into the formation of silver particles within PFPE/sc-CO_2 reverse micelles. These studies will investigate the formation of silver nanoparticles and silver intermediates within PFPE/sc-CO_2 reverse micelles as evidenced by multiple UV−vis absorption bands indicative of silver intermediates. We will show that silver intermediate stabilization is dependent upon a unique environment existing in the PFPE/sc-CO_2 reverse micelle. Specifically, we will demonstrate the effect of reducing agent, water content, water core buffering, water core acidity, PFPE surfactant presence, and the addition of cosurfactants such as AOT on the stabilization of silver intermediates and silver nanoparticles.

Experimental Section

Materials. The surfactant sodium bis(2-ethylhexyl) sulfosuccinate (AOT) and certified 10 N sodium hydroxide (NaOH) buffer were purchased from Fisher Scientific. Sodium borohydride 99% ($NaBH_4$) and silver nitrate 99.9999% ($AgNO_3$) were purchased from Aldrich. Sodium triacetoxyborohydride 97% reducing agent and isooctane (HPLC-grade) were acquired from Acros. Carbon dioxide was obtained from BOC Gases. Deionized water was used in all experiments requiring water. The ammonium carboxylate perfluoropolyether of general formula $X[CF_2CF(CF_3)O]_nCF_2COO^-NH_4^+$ (where X is CF_3O or Cl) and average molecular weight of 667 (for X = CF_3O) or 632 (for X = Cl) with the structure shown in Figure 2 was synthesized according to previously reported methods.[35] The acid form of PFPE as received from Ausimont was neutralized with a 10-fold molar excess of ammonium hydroxide. Following neutralization, the surfactant was then dried in a vacuum oven at 40 °C for 48 h. Experiments were initially conducted with completely fluorinated PFPE, but use of the PFPE containing chlorine was eventually necessitated by commercial availability. Use of ammonium-functionalized PFPE surfactant in either completely fluorinated (PFPE-NH_4) or chlorine-containing form (Cl-PFPE-NH_4) is designated in the discussion.

A silver-functionalized Cl-PFPE (Cl-PFPE-Ag) was synthesized according to Bio-Rad Labs recommendations (D. Hardy, personal communication, June 2001) by adding 14.8 N ammonium hydroxide (NH_4OH) to the carboxylic acid form of Cl-PFPE until a pH of 4.5 was achieved. The pH was elevated to provide a pK_a appropriate for silver exchange with the acidic hydrogen. Subsequently, a 2 M aqueous $AgNO_3$ solution was added to the mixture for a maximum fractional exchange of approximately 30%. The solution was allowed to mix for 14 h, after which time the mixture was finally neutralized with NH_4OH. The surfactant was then dried in a vacuum oven for 48−72 h at 40 °C.

Particle Formation. The reactions were performed in a constant volume (96 mL) stainless steel reactor fitted with two quartz windows for UV−vis analysis and compartmentalized with stainless steel valves and fittings. A PTFE insert capable of holding an additional quartz window was used in some circumstances to reduce the optical path length from 3.2 to 1.9

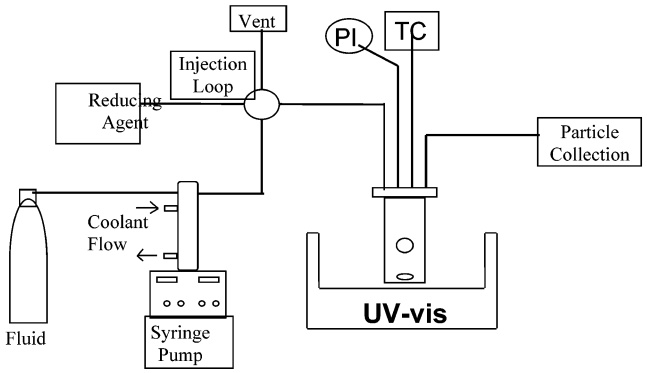

Figure 1. Schematic of experimental apparatus.

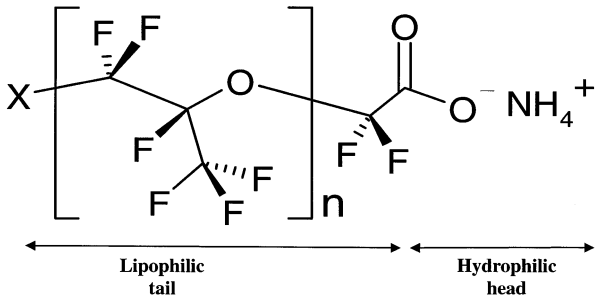

Figure 2. Structure of ammonium-functionalized perfluoropolyether surfactant (NH_4-PFPE) where X is either F or Cl.

cm. The window and PTFE insert reduced the vessel volume to 87 mL. A schematic of the experimental apparatus is presented in Figure 1. Desired amounts of surfactant, silver nitrate, deionized water, and NaOH (where noted) were initially loaded into the vessel. Details of concentrations for specific experiments are listed in the Results and Discussion. The bulk solvent (e.g., CO_2) was then injected into the vessel with an Isco 260D high-pressure syringe pump until the desired pressure was achieved. Vessel contents were allowed to mix for several hours at the desired temperature and pressure. A known amount of reducing agent was displaced into the vessel with bulk solvent via the Isco syringe pump and an external injection loop. Stirring was ceased following addition of the reducing agent to allow particle growth to occur through a process of natural reverse micelle collision and exchange. Pressure within the vessel was monitored to within ±0.7 bar by use of a 68920-44 Psi-Tronix pressure gauge, and temperature was maintained to within 0.1 °C by use of a heating tape, platinum RTD, and an Omega CN76000 controller. A UV−vis baseline was recorded for each experiment prior to reaction on a Varian 3E spectrophotometer. Particle growth could then be monitored by collecting UV−vis spectra as a function of time.

Nanoparticles of metallic silver were produced in compressed liquid propane at 37 °C, 200 bar, and a *W* of 10 with AOT, $AgNO_3$, and $NaBH_4$ concentrations of 100, 1, and 3 mM, respectively. Synthesis of silver particles in water-in-CO_2 reverse micelles was accomplished at temperatures between 36 and 37 °C, pressures ranging from 200 to 325 bar, and molar water-to-surfactant ratios, *W*, between 0 and 10. The *W* values reported in this paper are uncorrected for the slight solubility of water in carbon dioxide, which would slightly decrease the localized water content. As an example, for a 2 wt % (30 mM) PFPE-NH_4 system, a *W* of 12 would result in a corrected *W* of approximately 8.5 based on the solubility of water in pure CO_2 at 3000 psi and 37 °C.[36] It should be noted that this corrected *W* is based on the solubility of H_2O in pure CO_2. Unfortunately, the partitioning of H_2O between CO_2 and the reverse micelle

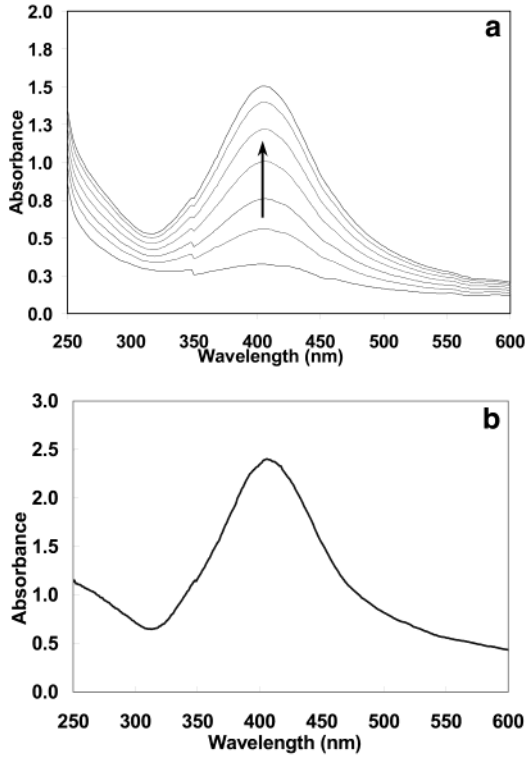

Figure 3. UV−vis absorption spectra indicative of silver nanoparticles (a) growing as a function of time in AOT/isooctane with $W = 10$, $T = 25$ °C, $P = 1$ bar, [AOT] = 100 mM, [$AgNO_3$] = 1 mM, and [$NaBH_4$] = 3 mM and (b) present in AOT/propane reverse micelles with $W = 10$, $T = 37$ °C, $P = 200$ bar, [AOT] = 100 mM, [$AgNO_3$] = 1 mM, and [$NaBH_4$] = 3 mM.

cores has not been measured, and as such we report the uncorrected *W* value. The PFPE concentrations ranged between 1.4 wt % (20 mM) and 2.2 wt % (30 mM) while $AgNO_3$ concentrations ranged from 0.4 to 1.1 mM. Reducing agent concentrations extended from 0.5 to 3 mM for $NaBH_4$ and from 0.2 to 0.3 mM for $NaBH(OAc)_3$. Details relating to specific experiments are outlined in the following Results and Discussion section.

Transmission electron microscope analysis was performed on a Zeiss EM 10 TEM. Sample grids were prepared by either of two techniques. (1) The first method involves slow depressurization of the nanoparticle microemulsion, after which the surfactant mixture collects on the bottom of the vessel. The surfactant mixture containing the nanoparticles is next collected and redispered in ethanol. TEM grids of the nanoparticles could then be prepared by placing a drop of ethanol/particle mix on a nickel grid. (2) Rapid expansion of the supercritical solvent (RESS) constituted a less intrusive and more effortless method for particle dispersion onto a surface such as a TEM grid. This technique consisted of rapid expansion of the reactor contents through a 100 μm capillary tube onto a TEM grid. These particles can then be directly analyzed on a TEM, though no further UV−vis spectra are attainable.

Results and Discussion

Ag in Liquid AOT/Alkane Systems. Previous studies have shown the feasibility of silver nanoparticle production within reverse micelles by use of the surfactant sodium bis(2-ethylhexyl) sulfosuccinate (AOT). Figure 3a shows the characteristic absorption spectra of silver nanoparticles synthesized from silver nitrate reduction by sodium borohydride ($NaBH_4$) within the water core of AOT reverse micelles in liquid

isooctane. The figure demonstrates the typical decrease in bandwidth and increase in peak intensity as reaction time proceeds.[14] The peak full width at half maximum has been found to vary linearly with the inverse of the particle diameter, thus providing a valuable method of in situ particle size characterization.[14] As shown in Figure 3b, the same characteristic peak results for silver nanoparticles formed in compressed propane when the surfactant AOT and the reducing agent sodium borohydride are used. The silver nanoparticles were synthesized in compressed propane at 37 °C, 200 bar, and a W of 10 with AOT, $AgNO_3$, and $NaBH_4$ concentrations of 100, 1, and 3 mM.

Ag in PFPE-NH_4/sc-CO_2 Systems. Having produced nanoparticles by reverse micelles in alkane solvents and given that the formation of reverse micelles in sc-CO_2 is possible through the use of PFPE surfactant, it would appear that production of nanoparticles in PFPE/CO_2 reverse micelles would be straightforward. The ammonium-functionalized PFPE surfactant previously described was used as a replacement for AOT in order to create a stable water/sc-CO_2 microemulsion. However, as Figure 4a clearly shows, extension of the micelle system to supercritical carbon dioxide resulted in behavior inconsistent with the previous trend of one plasmon centered at 400 nm. Rather than the characteristic absorption spectra indicative of silver nanoparticles, multiple absorption bands were obtained at various locations. Interestingly, the bands persist for extensive periods of time (shown to 9 h), indicating stabilization of some unexpected product.

The initial experiment employed sodium borohydride as the reducing agent; thus the possibility existed that the sodium borohydride reducing agent was the source of the multiple absorption bands, be they from incomplete silver reduction or byproduct formation with carbon dioxide. To elucidate the relationship of reducing agent to formation of multiple absorption bands, the sodium borohydride reducing agent was replaced by sodium triacetoxyborohydride [$NaBH(OAc)_3$], which has been reported to be less reactive toward carbon dioxide.[32] Panels b and c of Figure 4 present typical spectra obtained for silver particles produced with the alternate reducing agent $NaBH(OAc)_3$. The new reducing agent produces an increased absorbance, which may indicate less reaction with CO_2 and greater reduction of Ag^+. However, multiple UV−vis peaks, specifically located at 275, 350, 380, 420, 470, and 530 nm, still persist for long periods of time.

Furthermore, an experiment was performed whereby reducing agent was injected into a system absent of silver nitrate, after which no absorption bands were observed. All together, this indicates that the reducing agent is not the sole cause of the multiple absorption bands and also that they are the consequence of some silver derivative. On the basis of findings by other researchers, who have seen similar peaks and have linked them to individual intermediates, the multiple absorption bands most likely indicate the presence of stabilized silver intermediates.

Absorption Band Identification. Many researchers have investigated silver particle formation on microsecond time scales and have identified silver intermediate UV−vis bands indicative of silver clusters composed of small numbers of atoms. UV−vis peak location may also result from particle shape, size, multiple particle environments, etc.[14,37]

The peak observed at 270 nm may indicate Ag_4^{2+} intermediates, as this location has been widely reported in the literature to denote Ag_4^{2+} presence. Henglein and Tausch-Treml[38] observed this intermediate at 260 nm and on the time scale of milliseconds in aqueous Ag_2SO_4 solution after a high-energy radiation pulse. Petit et al.[14] reported possible stabilization of

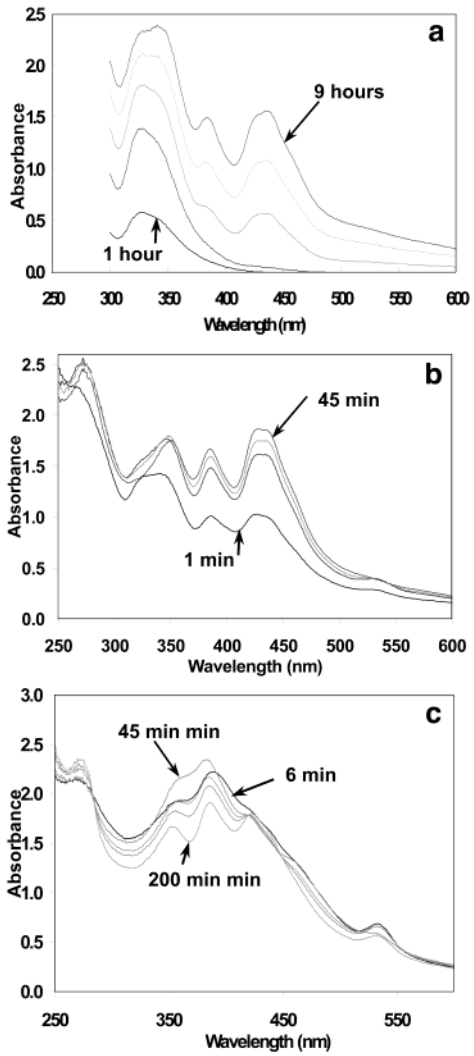

Figure 4. UV−vis absorption spectra showing multiple absorption bands at 270, 350, 380, 420, 470, and 530 nm following silver nitrate reduction in PFPE-NH_4/CO_2 reverse micelles by (a) sodium borohydride (3 mM) reducing agent with $W = 10$, $T = 37$ °C, $P = 275$ bar, [PFPE-NH_4] = 1.4 wt % (20 mM), and [$AgNO_3$] = 1.1 mM; (b) sodium triacetoxyborohydride (0.3 mM) reducing agent with $W = 8$, $T = 36$ °C, $P = 200$ bar, [Cl-PFPE-NH_4] = 2.2 wt % (30 mM), and [$AgNO_3$] = 0.8 mM; and (c) sodium triacetoxyborohydride (0.26 mM) reducing agent with $W = 10$, $T = 37$ °C, $P = 300$ bar, [Cl-PFPE-NH_4] = 2.0 wt % (30 mM), and [$AgNO_3$] = 0.4 mM.

Ag_4^{2+} as indicated by a peak at 275 nm utilizing AOT/isooctane reverse micelles with a low water content of $W \leq 1.5$. Furthermore, Zhang et al.[39] attributed a peak at 270 nm to Ag_4^{2+} formation in aqueous microemulsions.

The absorbance near 350 nm may be attributed to a wider range of intermediates. Metal silver atom (Ag^0) and oligomeric clusters are reported to absorb at 360 nm by Dimitrijevic et al.[40] They also found that a decay of dimer cation at 320 nm led to formation of the oligomeric clusters at 360 nm. These oligomeric clusters could then proceed to the formation of colloidal metallic silver particles. Additional bands at 310 and 345 nm have been ascribed to clusters consisting of Ag_9^+ and/or Ag_8^{2+}.[41] Henglein found that intermediates composed of these clusters could be stabilized by sodium polyacrylate chains of high carboxylate density. In some of our experiments the 350 nm peak can be seen to fall as the peak near 400 nm grows, which may indicate a large cluster such as Ag_9^+.

Plasmon absorption bands observed at 390 and 420 nm may indicate the presence of silver nanoparticles situated within

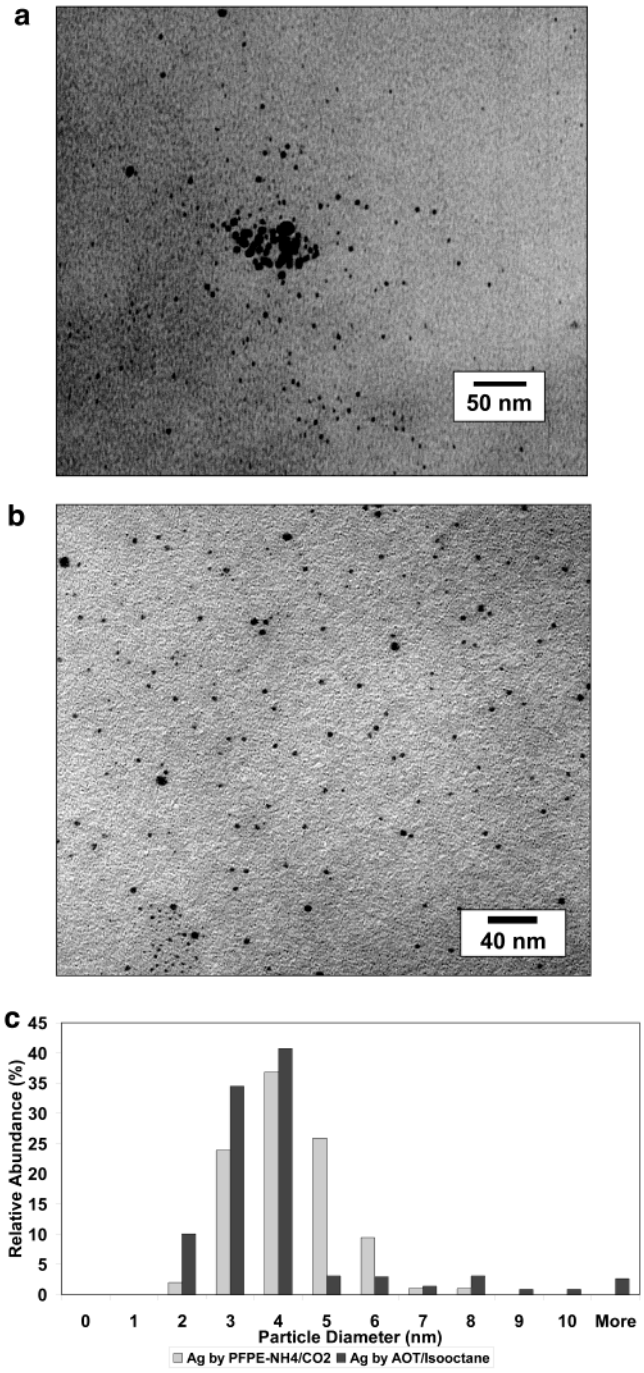

Figure 5. (a) TEM micrograph of silver particles produced in AOT/isooctane reverse micelles with $W = 10$, $T = 37$ °C, $P = 200$ bar, [AOT] = 100 mM, [$AgNO_3$] = 1 mM, and [$NaBH_4$] = 3 mM. (b) TEM image of silver particles synthesized in NH_4-PFPE/CO_2 reverse micelles at $W = 10$, $T = 35$ °C, $P = 250$ bar, [PFPE-NH_4] = 2.2 wt % (30 mM), [$AgNO_3$] = 1 mM, and [$NaBH(OAc)_3$] = 0.1 mM. (c) Corresponding mean particle diameter size distribution for each.

different regions. Metallic silver nanoparticles are commonly characterized by the absorption local to 400 nm. This absorbance varies between 380 and 420 nm depending upon the size, shape, and surrounding environment in which the nanoparticle is situated.[14,38,39] In light of this it is possible that the peaks observed at 390 and 420 nm are the result of silver nanoparticles situated in different microenvironments such as the acidic, bulk water, and polar surfactant headgroup regions observed by Johnston and co-workers,[19,20] when the methyl orange probe was used. It should be noted, however, that these regions were observed to be more pronounced as the water content of the reverse micelle was increased, particularly at W values greater than 17, whereas our system consisted of water loadings near $W = 10$. Furthermore, Zhang et al.[39] reported a blue shift of 7 nm, to 384 nm, for silver nanoparticles near polyacrylate when compared to the absorbance measured in bulk water. Ershov and Henglein[41] also reported the wavelength of maximum absorbance to depend on the particle size, whereby larger silver nanoparticles are located at 420 nm. Therefore, there are many contributions that could result in the bands near 400 nm.

Bands measured in the 480 and 540 nm region are potential clusters of silver atoms and ions. Ershov and Henglein[41,42] performed a series of silver ion reductions using hydrated electrons in aqueous polyacrylate solution, which allowed for observation of monatomic and nanometer-sized clusters, thereby giving details about intermediate cluster progression to silver nanoparticles. As such, they attributed a peak at 480 nm resulting from a condensation of dimeric silver complexes to form larger complexes consisting of about four silver atoms and an approximately equal number of silver ions. Zhang et al.[39] also accredited a peak at 540 nm to clusters probably larger than a Ag_4^{2+} dimer, consisting of approximately equal numbers of silver atoms and ions. This peak was observed in an experiment that used stopped-flow technique on the order of 70 ms to examine silver intermediates stabilized by polyacrylate in aqueous solution.

Ag Size Comparison in AOT/Alkane vs PFPE-NH_4/sc-CO_2 Systems. Transmission electron microscopy was used to obtain images of the silver nanoparticles on a carbon-coated nickel grid. Figure 5a shows particles created in an AOT/propane reverse micelle system. From micrographs obtained under these conditions, the size distribution in Figure 5c for AOT/propane particles was obtained, which indicates a mean particle diameter of approximately 3.8 nm with a 2.4 nm standard deviation. The particle size distribution was obtained by measuring the diameter of all of the particles (more than 720 particles) from six micrographs from different parts of the grid (×150000).

Figure 5b presents particles produced in PFPE/CO_2 reverse micelles. Applying the same technique to particles produced in the PFPE/CO_2 reverse micelles gives the second size distribution shown in Figure 5c. A total of 201 particles were counted to make up the size distribution, which shows a fairly even and narrow distribution of particles around 3.5 nm in diameter. Despite the presence of silver intermediates, which would likely be too small to appear on a TEM, the presence of monodisperse particles at comparable sizes to particles produced in compressed propane nevertheless demonstrates the feasibility of silver particle production in PFPE-NH_4/CO_2 reverse micelles.

Ag in Buffered PFPE-NH_4/sc-CO_2 Systems. As previously mentioned, micelles formed in supercritical CO_2 have acidic water cores, unlike the AOT/alkane microemulsion,. This results from CO_2 partitioning into and subsequent reaction with the water core to form carbonic acid:

$$CO_2 + H_2O \leftrightarrow H_2CO_3 \leftrightarrow H^+ + HCO_3^- \qquad (2)$$

Investigation by Niemeyer and Bright[43] using the fluorescent probe Cl-NERF identified the pH within PFPE/CO_2 reverse micelles to be between 3.1 and 3.5 while having relatively little relation to water loading or CO_2 solvent pressure. Since many reaction outcomes and equilibrium reactions rely strongly on pH, this presents an obstacle to the tunability of the micelle "nanoreactor". More recently, Holmes et al.[44] demonstrated the ability to buffer the water core to pH values approaching 7 using a number of bases, of which NaOH was the more effective.

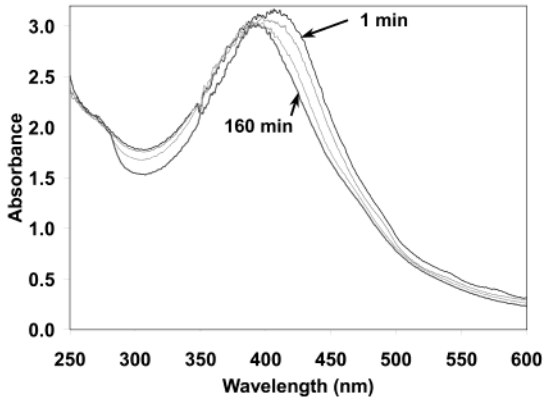

Figure 6. Absorption spectra of silver nanoparticles synthesized in elevated pH Cl-PFPE-NH_4/CO_2 microemulsion. An approximate pH of 6 was brought about by 0.5 M NaOH water buffering. System conditions were $W = 10$, $T = 37$ °C, $P = 240$ bar, [Cl-PFPE-NH_4] = 1.9 wt % (30 mM), [$AgNO_3$] = 0.6 mM, and [$NaBH(OAc)_3$] = 0.2 mM.

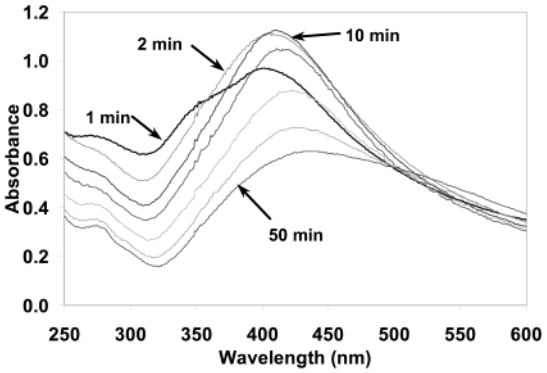

Figure 7. UV−vis spectra of silver nanoparticles produced from dry, silver-functionalized Cl-PFPE surfactant with $W = 0$, $T = 37$ °C, $P = 260$ bar, [Cl-PFPE-NH_4] = 2.0 wt % (30 mM), $[\text{Cl-PFPE-Ag}]_{max} = 0.26$ mM, and [$NaBH_4$] = 0.6 mM.

Using the results of the experimental measurements of Holmes et al., the reverse micelle water cores were buffered with the required amount of NaOH to achieve an approximate pH of 6. Following reduction, we obtained the absorption spectra shown in Figure 6 for metallic silver nanoparticles. Once again, the single absorption band indicating silver nanoparticles is evident at 400 nm. This indicates an effect of buffering upon intermediate stabilization in the reverse micelle system. The absence of strong multiple peaks at locations 360, 420, 470, and 550 nm may indicate a reduced concentration of Ag intermediates and an increased concentration of nanoparticle silver. It should be stressed that this destabilization may result from an unknown mechanism, such as NaOH ion interference or reaction with remaining Cl-PFPE carboxylic acids, rather than necessarily the raised core pH.

Ag in Ag-PFPE-NH_4/sc-CO_2 ($W = 0$) Systems. To further investigate the effect of the reverse micelle water core, an experiment was performed in which no additional water was added to the system, thus making "dry" reverse micelles. Since no water was present, carbon dioxide could not react to form carbonic acid. A small amount of silver-functionalized surfactant (Cl-PFPE-Ag) was used in conjunction with Cl-PFPE-NH_4 to load silver into the microemulsion. The silver was then reduced by sodium borohydride (0.0006 M in vessel) and monitored to give the absorption spectra shown in Figure 7. What is especially interesting is the spectrum measured after only 1 min, as peaks can be observed at 275, 350, and 400 nm. But after only one more minute, absorbances at 275 and 350 nm have diminished while the band at 410 nm has become more focused and intense. Typical of nanoparticle synthesis in reverse micelles, the single band temporarily grows in intensity and decreases in width before the onset of particle agglomeration and precipitation, which is indicated by the broadening and flattening of the spectrum. As a result, we can conclude that there is something special about the reverse micelle water core that facilitates silver intermediate stabilization, particularly at 275 and 350 nm.

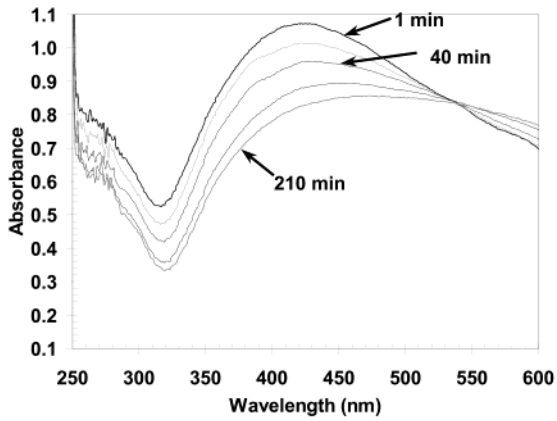

Figure 8. UV−vis spectra of silver nanoparticles produced in AOT/PFPE-NH_4/CO_2 reverse micelles. Conditions: $W = 12$, $T = 37$ °C, $P = 325$ bar, [PFPE-NH_4] = 1.8 wt % (30 mM), [AOT] = 12.8 mM, [$AgNO_3$] = 0.35 mM, and [$NaBH(OAc)_3$] = 0.4 mM.

Ag in PFPE-NH_4/AOT/sc-CO_2 Systems. The next experiment undertaken was addition of AOT to the NH_4-PFPE reverse micelles. A similar system has been reported by Ji et al.[32] using a mixture of AOT and PO_4-PFPE. Despite the different functional group on the PFPE surfactant, the spectrum we obtained coincides well with those obtained by Ji et al. The UV−vis spectrum for the reaction is presented in Figure 8 and demonstrates a wide bandwidth as well as an absorbance that decreases with time. Such spectra may denote polydisperse particles that tend to agglomerate and precipitate from solution as time progresses. If intermediate stabilization were entirely the result of low pH, then we should have seen multiple peaks regardless of the addition of AOT surfactant. Thus, this demonstrates that the PFPE/CO_2 environment is different from the AOT/PFPE/CO_2 environment such that the AOT, like the NaOH, is able to destabilize the intermediates of silver.

Ag in PFPE-NH_4/HFE Systems. The importance of carbon dioxide to intermediate stabilization was examined by use of a liquid hydrofluoroether (3M HFE 7100) in place of carbon dioxide. After the presence of reverse micelles having a bulk water environment was verified with the solvatochromic probe methyl orange, silver ions solvated in the reverse micelles were gradually reduced by incremental 1 μL additions of $NaBH_4$/water solutions. The microemulsion reducing agent concentration after each addition is displayed in the inset to Figure 9. The figure also shows UV−vis spectra recorded after reducing agent additions. Initially the spectra show low absorption with multiple peaks apparent at locations of 275, 350, 390, and 430 nm. Corresponding to incremental reductions, the peaks proceed to rise and fall in locations near those observed in CO_2 until a final single absorption band located at 400 nm persists. The water core pH in these HFE/ PFPE-NH_4 reverse micelles should no longer be acidic, since CO_2 is no longer present to form carbonic acid by reacting with the water. Despite this elevated pH, the multiple absorbance bands persist, thereby suggesting that the ammonium PFPE surfactant in the reverse micelle

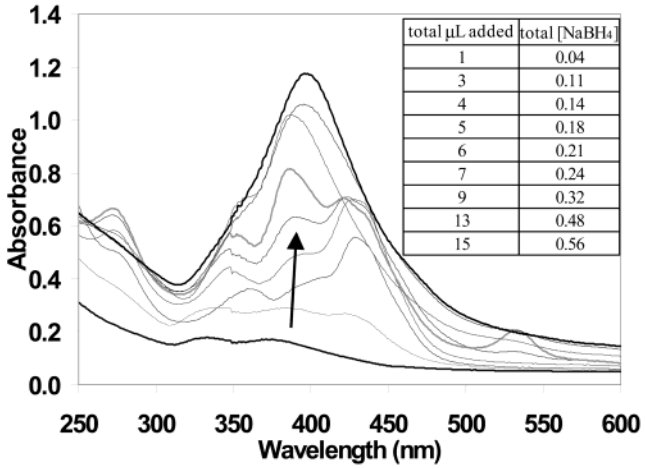

total μL added	total [$NaBH_4$]
1	0.04
3	0.11
4	0.14
5	0.18
6	0.21
7	0.24
9	0.32
13	0.48
15	0.56

Figure 9. UV−vis spectra of silver intermediates formed in Cl-PFPE-NH_4/HFE 7100 reverse micelles. The microemulsion consisted of 10 mL of HFE 7100, [Cl-PFPE-NH_4] = 0.8 wt % (20 mM), [$AgNO_3$] = 1.7 mM, and an initial *W* value of 10. Reducing agent concentrations (millimolar) after microliter solution additions are presented by the inset table.

environment plays a primary role in the stabilization of silver intermediates. These results also demonstrate that stabilization is not simply an effect of low pH, as might be apparent from the results obtained after CO_2 reverse micelles are buffered with NaOH. Rather, in addition to elevating the pH, the added base also provides a counterion that could disrupt the stabilizing interaction between the intermediate and the ammonium PFPE surfactant.

Conclusions

Nanometer-sized silver intermediates were formed by silver ion reduction in PFPE-NH_4 reverse micelles dispersed in bulk supercritical CO_2 solvent. UV−vis spectroscopy was used to monitor the nanoparticle growth, which, rather than showing the single characteristic absorbance at 400 nm for silver nanoparticles, indicated at least five multiple absorption bands. These multiple absorption bands are indicative of silver intermediate, and the persistence of the bands for extensive periods of time indicates a relatively unexpected phenomenon in reverse micelles.

The means of intermediate stabilization was attributed to an effect of the PFPE surfactant and the water core in the reverse micelle microenvironment. The reducing agent type and bulk CO_2 solvent were determined to have no effect on the intermediate stabilization. Substitution of reducing agents revealed that there was no effect on particle formation as well as indicating that no byproducts form by reaction with CO_2. Additionally, in the absence of silver salts within the reverse micelles, no absorption bands were observed upon addition of reducing agent, indicating that the multiple absorption bands are the result of some silver derivative. Reaction of silver-functionalized PFPE surfactant at $W = 0$ revealed a temporary absorbance near 350 nm in progression to a single characteristic absorbance of silver nanoparticles at 410 nm. This also suggests the importance of the water core to intermediate stabilization. TEM analysis of particles formed in the PFPE/CO_2 microemulsions showed monodisperse particles that were comparable in size to particles produced in AOT/propane reverse micelles, thus demonstrating the effective production of particles despite the formation of silver intermediates. Finally, substitution of the CO_2 bulk solvent by a hydrofluoroether solvent resulted in identical multiple absorption bands that were incrementally reduced to give a single characteristic absorption band for silver. This indicates that the PFPE-NH_4 surfactant in the reverse micelle water core environment plays a primary role in stabilizing the silver intermediates. Furthermore, the HFE experiment demonstrates that the bulk CO_2 solvent and low pH are not the primary causes of intermediate stabilization, since the HFE/PFPE-NH_4 water core is not acidic.

Acknowledgment. We thank Dr. Michael Miller of the Auburn University Biological Electron Microscopy Imaging Facility for his assistance with the TEM analysis. We also thank Professor German Mills (Auburn University), Kedar Khambaswadkar, and Joanna P. Cason for their technical support. In addition, we thank 3M for the donation of the HFE 7100 sample. This work was partially supported by a grant from The Department of Energy, Basic Energy Sciences (DE-FG02-01ER15255), and we appreciate their financial assistance.

References and Notes

(1) Jacobson, G. B.; Lee, C. T.; Johnston, K. P. *J. Org. Chem.* **1999**, *64*, 1201.
(2) Adair, J. H.; Li, T.; Kido, K.; Havey, K.; Moon, J.; Mecholsky, J.; Morrone, A.; Tlaham, D. R.; Ludwig, M. H.; Wang, L. *Mater. Sci. Eng.* **1998**, *R23*, 139.
(3) Pileni, M. P.; Lisiecki, I.; Motte, L.; Petit, C.; Cizeron, J.; Moumen, N.; Lixon, P. *Prog. Colloid Polym. Sci.* **1993**, *93*, 1.
(4) Pileni, M. P. *J. Phys. Chem.* **1993**, *97*, 6961.
(5) Harai, T.; Sato, H.; Komasawa, I. *Ind. Eng. Chem. Res.* **1994**, *33*, 3262.
(6) Cason, J. P.; Miller, M. E.; Thompson, J. B.; Roberts, C. B. *J. Phys. Chem. B* **2001**, *105*, 2297.
(7) (a) Cason, J. P.; Khambaswadkar, K.; Roberts, C. B. *Ind. Eng. Chem. Res.* **2000**, *39*, 4749. (b) Cason, J. P.; Roberts, C. B. *J. Phys. Chem. B* **2000**, *104*, 1217.
(8) Bagwe, R. P.; Khilar, K. C. *Langmuir* **1997**, *13*, 6432
(9) Bagwe, R. P.; Khilar, K. C. *Langmuir* **2000**, *16*, 905.
(10) Towey, T. F.; Khan-Lodhi, A.; Robinson, B. H. *J. Chem Soc., Faraday Trans.* **1990**, *86*, 3757.
(11) Lisiecki, I.; Lixon, P.; Pileni, M. P. *Prog. Colloid Polym. Sci.* **1991**, *84*, 342.
(12) Pileni, M. P.; Lisiecki, I. *Colloids Surf.* **1993**, *80*, 63.
(13) Lisiecki, I.; Pileni, M. P. *J. Phys. Chem.* **1995**, *99*, 5077.
(14) Petit, C.; Lixon, P.; Pileni, M. P. *J. Phys. Chem.* **1993**, *97*, 12974.
(15) McHugh, M. A.; Krukonis, V. J. *Supercritical Fluid Extraction, Priniciples and Practice*, 2nd ed.; Butterworth-Heinemann: Boston, MA, 1994.
(16) Matson, D. W.; Fulton, J. L.; Smith, R. D. *Mater. Lett.* **1987**, *6*, 31.
(17) Parag, S. S.; Holmes, J. D.; Johnston, K. P.; Korgel, B. A. *J. Phys. Chem. B* **2002**, *106*, 2545.
(18) Consani, K. A.; Smith, R. D. *J. Supercrit. Fluids* **1990**, *3*, 51.
(19) Johnston, K. P.; Harrison, K. L.; Clarke, M. J.; Howdle, S. M.; Heitz, M. P.; Bright, F. V.; Carlier, C.; Randolph, T. W. *Science* **1996**, *271*, 624.
(20) Clarke, M. J.; Harrison, K. L.; Johnston, K. P.; Howdle, S. M. *J. Am. Chem. Soc.* **1997**, *119*, 6399.
(21) Liu, Z.-T.; Erkey, C. *Langmuir* **2001**, *17*, 274.
(22) Harrison, K.; Goveas, J.; Johnston, K. P.; O'Rear, E. A. *Langmuir* **1994**, *10*, 3536.
(23) Zielinski, R. G.; Rosov, N.; Kaler, E. W.; Kline, S. R. *Langmuir* **1997**, *13*, 3934.
(24) Eastoe, J.; Cazelles, B. M. H.; Steytler, D. C.; Holmes, J. D.; Pitt, A. R.; Wear, T. J.; Heenan, R. K. *Langmuir* **1997**, *13*, 6980.
(25) Holmes, J. D.; Steytler, D. C.; Rees, G. D.; Robinson, B. H. *Langmuir* **1998**, *14*, 6371.
(26) Jacobson, G. B.; Lee, C. T.; Johnston, K. P. *J. Org. Chem.* **1999**, *64*, 1201.
(27) Heitz, M. P.; Carlier, C.; deGrazia, J.; Harrison, K. L.; Johnston, K. P.; Randolph, T. W.; Bright, F. V. *J. Phys. Chem. B* **1997**, *101*, 6707.
(28) da Rocha, S. R. P.; Johnston, K. P. *Langmuir* **2000**, *16*, 3690.
(29) Lee, C. T.; Johnston, K. P.; Dai, H. J.; Cochran, H. D.; Melnichenko, Y. B.; Wignall, G. D. *J. Phys. Chem. B* **2001**, *105*, 3540.
(30) Zielinski, R. G.; Kline, S. R.; Kaler, E. W.; Rosov, N. *Langmuir* **1997**, *13*, 3934.
(31) Holmes, J. D.; Bhargava, P. A.; Korgel, B. A.; Johnston, K. P. *Langmuir* **1999**, *15*, 6613.

(32) Ji, M.; Chen, X.; Wai, C. M.; Fulton, J. L. *J. Am. Chem. Soc.* **1999**, *121*, 2631.

(33) Ohde, H.; Rodriguez, J. M.; Ye, X.; Wai, C. M. *Chem. Commun.* **2000**, *23*, 2353.

(34) Ohde, H.; Hunt, F.; Wai, C. M. *Chem. Mater.* **2001**, *13*, 4130.

(35) Holmes, J. D.; Ziegler, K. J.; Audriani, M.; Lee, C. T.; Bhargava, P. A.; Steytler, D. C.; Johnston, K. P. *J. Phys. Chem. B* **1999**, *103*, 5703.

(36) Wiebe, R. *Chem. Rev.* **1941**, *29*, 475.

(37) Andrews, M. P.; Ozin, G. A. *J. Phys. Chem.* **1986**, *90*, 2929.

(38) Henglein, A.; Tausch-Treml, R. *J. Colloid Interface Sci.* **1981**, *80*, 84.

(39) Zhang, Z.; Patel, R. C.; Kothari, R.; Johnson, C. P.; Friberg, S. E.; Aikens, P. A. *J. Phys. Chem. B* **2000**, *104*, 1176.

(40) Dimitrijevic, N. M.; Bartels, D. M.; Jonah, C. D.; Takahashi, K.; Rajh, T. *J. Phys. Chem. B* **2001**, *105*, 954.

(41) Ershov, B. G.; Henglein, A. *J. Phys. Chem. B* **1998**, *102*, 10663.

(42) Ershov, B. G.; Henglein, A. *J. Phys. Chem. B* **1998**, *102*, 10667.

(43) Niemeyer, E. D.; Bright, F. V. *J. Phys. Chem. B* **1998**, *102*, 1474.

(44) Holmes, J. D.; Ziegler, K. J.; Audriani, M.; Lee, C. T.; Bhargava, P. A.; Steytler, D. C.; Johnston, K. P. *J. Phys. Chem. B* **1999**, *103*, 5703.